Planar Layered Media Closed-form Green's Functions as a Series of Cylindrical Waves

David González Ovejero*, Francisco Mesa†, and Christophe Craeye‡

*Information Engineering Department, University of Siena, 53100 Siena, Italy, Email: gonzalez@dii.unisi.it
†Microwaves Group, Universidad de Sevilla, 41012 Sevilla, Spain, Email: mesa@us.es
‡ICTEAM Institute, Université catholique de Louvain, 1348 LLN, Belgium, Email: christophe.craeye@uclouvain.be

I. Introduction

The design of printed circuits and antennas remains a subject of intense research; it has fostered the development of efficient techniques for the analysis of structures in a planarly layered media. Among the available analysis tools, those based on a Mixed-Potential Integral Equation (MPIE) formulation and the Method of Moments (MoM) [1] are widely used. Actually, many commercial softwares extensively used in the analysis and design of planar circuits and antennas are based on this approach. When applying this technique, the discretization can be limited to the metalizations thanks to the use of appropriate Green's functions (GFs). Normally, in electrically large problems, one resorts to iterative techniques to solve the $N_T{\times}N_T$ dense system of equations in the MoM. In that case, the operation count for one iteration, which involves a matrix-vector product, scales as $\mathcal{O}(N_T^2)$. The evaluation of these matrix-vector products can be accelerated combining the Fast Multipole Method (FMM) with the Discrete Complex Image Method (DCIM) as in [2]. This strategy allows for the reduction of the computational cost of matrix-vector products to $\mathcal{O}(N_T^{3/2})$. Moreover, $\mathcal{O}(N_T \log N_T)$ operations per iteration can be achieved using either the Multilevel Fast Multipole Algorithm (MLFMA) together with the DCIM [3] or the Fast Inhomogeneous Plane Wave Algorithm (FIPWA) [4]. Finally, in [5] the Perfectly Matched Layer (PML)–MoM is combined with the MLFMA to achieve a $\mathcal{O}(N_T \log N_T)$ operation count for the matrix-vector products necessary at each iteration step.

One of the key points in the aforementioned techniques is the decomposition of the layered medium Green's functions (GFs) in closed-forms that allow one to exploit specific wave decompositions for the acceleration of the MoM problem. The most spread approach consists of using the DCIM to write the GF as a combination of spherical and cylindrical waves [2]. In [5], on the other hand, the introduction of a PML backed by a perfect electric conductor and placed above the layered medium limits the representation to a series of cylindrical waves. Using just cylindrical waves for the decomposition presents a clear advantage. As explained in [6, Sec. IV.C], the computational complexity of evaluating the MoM reaction integrals grows as $\mathcal{O}((kd)^2)$ (with k the wavenumber and d the radius of the smallest sphere containing the domain) for the spherical waves and as $\mathcal{O}(kd)$ for the cylindrical ones. Hence, the spatial domain GF expressed in closed-form as a sum of a limited number of cylindrical waves will reduce the computational burden. The rest of this paper explores two possibilities to achieve this goal.

II. Closed-form Green's Functions for Efficient Multipole Expansions

An accurate representation of the spectral domain Green's function can be obtained using exponential series, following the DCIM [2], or rational functions, applying PML-MoM or the Rational Function Fitting Method (RFFM). Rational functions are preferred to exponentials in this work, since they correspond to cylindrical waves in the spatial domain; and RFFM is preferred to PML-MoM, since it avoids the use of a perfectly matched layer. In the following, we will study the performance of two RFFM formulations for the well-known case of the Sommerfeld identity. If one assumes that source and observation points are in a common plane, it can be written as

$$\frac{\mathrm{e}^{-\mathrm{j}k\rho_{ij}}}{4\pi\rho_{ij}} = \frac{1}{4\pi}\frac{1}{2\mathrm{j}}\int_{-\infty}^{\infty}\frac{1}{k_z}H_0^{(2)}(k_\rho\,\rho_{ij})k_\rho \mathrm{d}k_\rho \tag{1}$$

where ρ_{ij} is the distance between source and observation points, $k_z=(k_\rho^2-k^2)^{1/2}$ and $H_0^{(2)}(\cdot)$ is the Hankel function of second kind and zero order. Hence, one may fit $1/k_z$ in pole-residue form as follows

$$\frac{1}{k_z} \approx \sum_{h=1}^{N_h}\frac{b_h}{k_\rho^2-q_h^2}\,, \tag{2}$$

where N_h is the number of cylindrical waves used and it is expected to govern the accuracy and range of validity of (4).

The coefficients b_h and q_h can be computed as in [7] or as explained in [8]. In the first case, the fitting coefficients are obtained by applying the method of Total Least Squares (TLS), any other implementation of the least square algorithm could also be applied. Instead, [8] uses a modified version of the VECTFIT algorithm in [9] with a particular weighting and combined with proper sampling paths. Although both implementations have identical goals, the TLS method in [7] and VECTFIT in [8] differ in several aspects. First, the TLS method provides b_h and q_h in one step, whereas the VECTFIT algorithm carries out an iterative search. Second, the TLS method applied to (2) forces the equality at $2N_h+3$ points

978-88-907018-1-8/13/$31.00 ©2013 IEEE

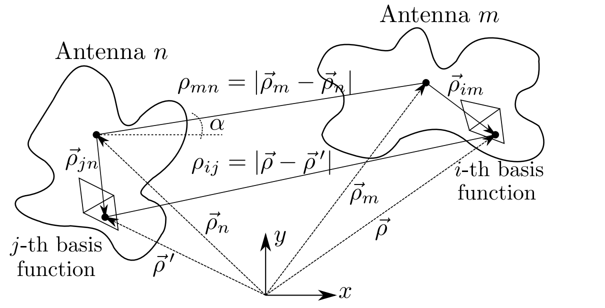

Fig. 1. Geometry considered for the multipole decomposition of the terms $H_0^{(2)}(q_h\,\rho_{ij})$.

(usually $N_h \sim 10$) of a sampled path in the complex k_ρ-plane. This path detours around the branch-point singularity and asymptotically approaches the real axis [7, eq. (11)]. On the other hand, the VECTFIT algorithm in [8] requires the sampling of a number of points (typically 10^3) substantially larger than $2N_h + 3$. Hence, the time devoted to one iteration in the VECTFIT algorithm will be larger than the total time required by the TLS method. The sampling points in the VECTFIT described in [8] can be uniformly or non-uniformly sampled along a path parallel to the real axis of the k_ρ-plane, with a small imaginary component [8, eq. (7)]. Indeed, the position of the sampling points in the complex k_ρ-plane will determine the approximation's range of validity in the spatial-domain. For instance, a set of uniformly spaced points used to sample the spectral domain GF for relative small values of k_ρ captures the intermediate field behavior of the GF. Its iterative nature and the number of high number sampling points make VECTFIT approach more flexible than TLS, as it is shown Section III. Conversely, TLS provides a more compact representation for a typical electrical size of the object to be analyzed.

Then, taking into account that

$$\int_{-\infty}^{\infty} \frac{1}{k_\rho^2 - q_h^2} H_0^{(2)}(k_\rho \rho) k_\rho \mathrm{d}k_\rho = -\mathrm{j}\pi H_0^{(2)}(q_h k_\rho) \quad (3)$$

one can write

$$\frac{\mathrm{e}^{-\mathrm{j}k\rho_{ij}}}{4\pi\rho_{ij}} \approx -\frac{1}{8}\sum_{h=1}^{N_h} b_h\, H_0^{(2)}(q_h\,\rho_{ij}) \quad (4)$$

After introducing the multipole expansion for the Hankel functions [6, eq. (11)] into (4), it becomes

$$\frac{\mathrm{e}^{-\mathrm{j}k\rho_{ij}}}{4\pi\rho_{ij}} \approx -\frac{1}{16\pi}\sum_{h=1}^{N_h} b_h \int_0^{2\pi} \mathrm{e}^{\mathrm{j}\,q_h\hat{\alpha}\cdot\vec{\rho}_{jn}}\,\mathrm{e}^{-\mathrm{j}\,q_h\hat{\alpha}\cdot\vec{\rho}_{im}} \times T^{\mathrm{2D}}(q_h, \vec{\rho}_{mn}, \alpha)\,\mathrm{d}\alpha \quad (5)$$

where the angles α are the integration points considered over the unit circumference, $\hat{\alpha} = \cos\alpha\,\hat{x} + \sin\alpha\,\hat{y}$, vector $\vec{\rho}_{jn}$ points from the center of the source domain n to the source point $\vec{\rho}_j$, $\vec{\rho}_{im}$ points from the center of the test domain m to the observation point $\vec{\rho}_i$, $\vec{\rho}_{mn}$ goes from the center of domain n to the center of domain m (see Fig. 1). Finally, $T^{\mathrm{2D}}(\cdot)$ is the translation operator defined as

$$T^{\mathrm{2D}}(p_h, \vec{\rho}_{mn}, \alpha) = H_0^{(2)}(p_h\,\rho_{mn}) + \sum_{q=1}^{Q} H_q^{(2)}(p_h\,\rho_{mn}) \cos\left[q(\phi_{mn} - \alpha)\right] \quad (6)$$

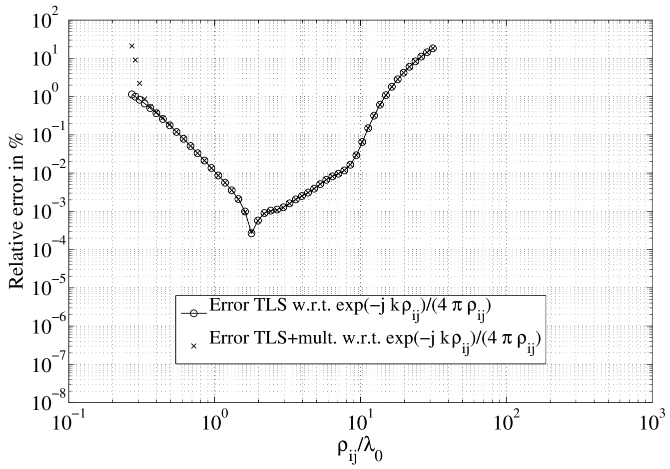

Fig. 2. Relative error (in %) for the values obtained using (4) and (4)+(5) with $N_h = 8$ w.r.t. the values obtained evaluating the left-hand side of (1), vs ρ_{ij}/λ_0.

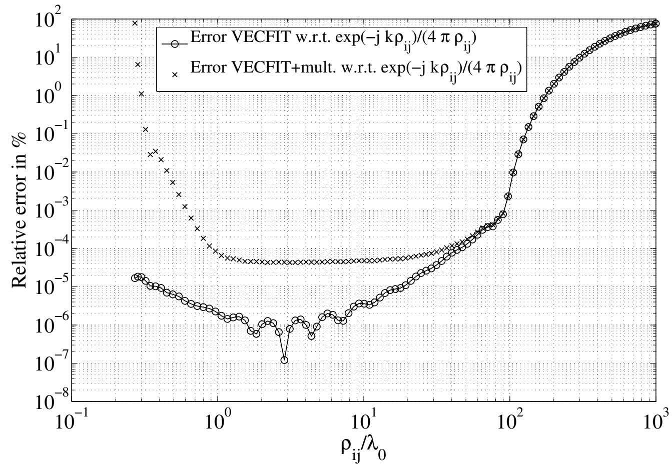

Fig. 3. Relative error (in %) for the values obtained using (4) and (4)+(5) with $N_h = 20$ w.r.t. the values obtained evaluating the left-hand side of (1), vs ρ_{ij}/λ_0.

The integration in (5) requires $\mathcal{O}(kd)$ quadrature points. Thus, the spherical wave term in (1) can be expressed as an equivalent sum of cylindrical waves, whose multipole expansion is computationally cheaper than the one of the corresponding spherical wave as long as $N_h < (kd)$.

III. Numerical results

In this section the accuracy and range of validity for (3) and (4) are addressed with a simple example. We consider an increasing horizontal distance between two points located on the $x - y$ plane in a homogeneous medium with $\epsilon_r = 2.7$. The distance of the source point to the domain center is $\rho_{jn} = \lambda_0/4\,\hat{x}$, and for the test point $\rho_{im} = -\lambda_0/4\,\hat{y}$, where λ_0 is the free-space wavelength. Fig. 2 shows the relative errors (in %) obtained using (4) and (5) with respect to the actual values, N_h is equal to 8 in this initial case. One can observe that the TLS+multipoles error remains below 0.1% from $0.5\lambda_0$ to $10\lambda_0$. On the other hand, the VECTFIT+multipoles approach (using the second sampling path proposed in [8, eq.(7)] with 10^3 sampling points) required 10 cylindrical waves to achieve a similar precision in that range of distances, which would lead to higher computational complexities in MoM problems. Nevertheless, one can easily increase the range of validity and precision by increasing N_h in VECTFIT, whereas this is more complicated with TLS due to some stability problems. Indeed, if one maintains the VECTFIT sampling path and increases N_h to 20, the VECTFIT+multipoles error remains below 0.1% from $0.3\lambda_0$ to $100\lambda_0$ (see Fig. 3).

IV. Conclusion

We have pointed out the advantages of writing the spatial domain Green's functions for a planar layered medium as a sum of cylindrical waves. Such a representation allows for multipole expansions with complexity $\mathcal{O}(kd)$ (with k the wavenumber and d the radius of the smallest sphere containing the domain), as opposed to the $\mathcal{O}((kd)^2)$ dependence found for spherical waves. Two modalities of the Rational Function Fitting Method (TLS and VECTFIT) are explored, and the pros and cons of each of them are briefly summarized. In the first instance, TLS appears to be more convenient to have N_h small, although VECTFIT offers more flexibility if one wants to increase the larger distance at which this approximation is valid.

References

[1] J. R. Mosig, "Integral equation technique," in *Numerical Techniques for Microwave and Millimeter-Wave Passive Structures*, T. Itoh, Ed. New York: Wiley, 1989, pp. 133–213.

[2] P. A. MacDonald and T. Itoh, "Fast simulation of microstrip structures using the fast multipole method," *Int. J. Numer. Modell. Electron. Networks Devices Fields*, vol. 9, no. 5, pp. 345–357, 1996.

[3] F. Ling, J. Song, and J.-M. Jin, "Multilevel fast multipole algorithm for analysis of large-scale microstrip structures," *IEEE Microw. Guided Wave Lett.*, vol. 9, no. 12, pp. 508–510, Dec. 1999.

[4] B. Hu and W. Chew, "Fast inhomogeneous plane wave algorithm for scattering from objects above the multilayered medium," *IEEE Trans. Geosci. Remote Sens.*, vol. 39, no. 5, pp. 1028–1038, May 2001.

[5] D. Vande Ginste, E. Michielssen, F. Olyslager, and D. De Zutter, "An efficient perfectly matched layer based multilevel fast multipole algorithm for large planar microwave structures," *IEEE Trans. Antennas Propag.*, vol. 54, no. 5, pp. 1538–1548, May 2006.

[6] D. González-Ovejero, F. Mesa, and C. Craeye, "Accelerated macro basis functions analysis of finite printed antenna arrays through 2D and 3D multipole expansions," *IEEE Trans. Antennas Propag.*, vol. 61, no. 2, Feb. 2013.

[7] R. R. Boix, F. Mesa, and F. Medina, "Application of total least squares to the derivation of closed-form Green's functions for planar layered media," *IEEE Trans. Microw. Theory Tech.*, vol. 55, no. 2, pp. 268–280, Feb. 2007.

[8] T. Kaifas, "Direct rational function fitting method for accurate evaluation of sommerfeld integrals in stratified media," *IEEE Trans. Antennas Propag.*, vol. 60, no. 1, pp. 282–291, Jan. 2012.

[9] V. Kourkoulos and A. Cangellaris, "Accurate approximation of Green's functions in planar stratified media in terms of a finite sum of spherical and cylindrical waves," *IEEE Trans. Antennas Propag.*, vol. 54, no. 5, pp. 1568–1576, May 2006.